J Fluoresc (2013) 23:41–47
DOI 10.1007/s10895-012-1114-5

ORIGINAL PAPER

Feasibility Study on Quantitative Measurements of Singlet Oxygen Generation Using Singlet Oxygen Sensor Green

Huiyun Lin · Yi Shen · Defu Chen · Lisheng Lin · Brian C. Wilson · Buhong Li · Shusen Xie

Received: 4 March 2012 / Accepted: 30 July 2012 / Published online: 23 August 2012

Abstract The purpose of this study is to investigate the feasibility for quantitative measurement of singlet oxygen ($^1O_2$) generation by using a newly developed $^1O_2$-specific fluorescence probe Singlet Oxygen Sensor Green reagent (SOSG). $^1O_2$ generation from photoirradiation of a model photosensitizer Rose Bengal (RB), in initially air-statured phosphate buffered saline (PBS) was indirectly monitored with SOSG. In the presence of $^1O_2$, SOSG can react with $^1O_2$ to produce SOSG endoperoxides (SOSG-EP) that emit strong green fluorescence with the maximum at 531 nm. The green fluorescence of SOSG-EP is mainly dependent on the initial concentrations of RB and SOSG, and the photoirradiation time for $^1O_2$ generation. Furthermore, kinetic analysis of the RB-sensitized photooxidation of SOSG is performed that, for the first time, allows quantitative measurement of $^1O_2$ generation directly from the determination of reaction rate. In addition, the obtained $^1O_2$ quantum yield of porphyrin-based photosensitizer hematoporphyrin monomethyl ether (HMME) in PBS by using SOSG is in good agreement with the value that independently determined by using direct measurement of $^1O_2$ luminescence. The results of this study clearly demonstrate that the quantitative measurement of $^1O_2$ generation using SOSG can be achieved by determining the reaction rate with an appropriate measurement protocol.

Keywords Singlet oxygen · Fluorescence probe · Singlet Oxygen Sensor Green reagent (SOSG) · Quantitative measurement · Luminescence · Quantum yield

Introduction

Singlet oxygen ($^1O_2$), the lowest excited electronic state of molecular oxygen, is a highly oxidative reactive oxygen species (ROS) that plays an important role in numerous chemical and photochemical reactions in different biological systems and, in particular, in photodynamic therapy (PDT) of solid tumors, age-related macular degeneration, localized infection and several benign skin conditions [1–3]. This had driven intense interest in $^1O_2$ measurements, and several physical and chemical methods have been reported [4–8]. The luminescence method, based on detection of the near-infrared (NIR) emission of $^1O_2$ around 1270 nm ($^1O_2 \rightarrow {}^3O_2$) has become a gold standard technique, particularly for PDT dosimetry, since it is direct and does not depend on any secondary reporters [4]. However, despite recent advances in high-sensitivity NIR photomultiplier tube (PMT) and single photon counting instrumentation, the technique remains technically challenging in biological systems, due to the weak signal that results from the very high reactivity of $^1O_2$ which means that only about 1 in 10^8 $^1O_2$ molecules undergoes luminescence deactivation [9, 10]. Hence, a variety of fluorescence probes have been developed to monitor $^1O_2$ generation indirectly with the objective of high selectivity, high sensitivity and easy detection, and the quantitative measurement of $^1O_2$ generation has been previously achieved by using DPAXs, DMAX, PATA-Tb^{3+} and MTTA-Eu^{3+}, respectively [11–13].

Electronic supplementary material The online version of this article (doi:10.1007/s10895-012-1114-5) contains supplementary material, which is available to authorized users.

H. Lin · Y. Shen · D. Chen · L. Lin · B. Li (✉) · S. Xie (✉)
Key Laboratory of OptoElectronic Science and Technology for Medicine of Ministry of Education, Fujian Provincial Key Laboratory for Photonics Technology, Fujian Normal University, Fujian 350007, China
e-mail: bhli@fjnu.edu.cn
e-mail: ssxie@fjnu.edu.cn

B. C. Wilson
Department of Medical Biophysics, University of Toronto/Ontario Cancer Institute, Toronto, Ontario M5G 2M9, Canada

The fluorescence probe, Singlet Oxygen Sensor Green reagent (SOSG), became commercially available in 2004. It has the advantage of being highly selective for $^1O_2$, versus other ROS such as the hydroxyl radicals or superoxide [14]. Most recently, Ogilby's group has independently illustrated the chemical structure of SOSG for its mechanistic studies [15]. As shown in Fig. 1, in the presence of $^1O_2$, SOSG can react with $^1O_2$ to produce SOSG endoperoxides (SOSG-EP) that are strongly fluorescence [16]. With a broad excitation peak around 510 nm, the fluorescence of SOSG-EP has the emission peak at 525-536 nm [14–17], which can be readily detected by a conventional PMT.

To date, SOSG has been successfully applied to monitor $^1O_2$ generation in a range of biological systems, including studies of light-activated plant defenses [16, 18], plasmonic engineering [19, 20], photoinactivation of bacterial viruses [21], photodegradation of 5-methyltetrahydrogolate [22] and photosensitizer-based PDT [23–26]. However, the feasibility for quantitative measurement of $^1O_2$ generation with SOSG has not been explored, and this is the focus of the present work, for which Rose Bengal (RB) that has been used in many photosensitization studies and has a high $^1O_2$ quantum yield of 0.76 in aqueous solution [27], was selected as a model photosensitizer. Furthermore, kinetic analysis of the RB-sensitized photooxidation of SOSG is performed to obtain the reaction rate, which allows the quantitative measurement of $^1O_2$ generation. In addition, we compare the $^1O_2$ quantum yields of porphyrin-based photosensitizer hematoporphyrin monomethyl ether (HMME) that determined by using SOSG as a fluorescent reporter and by using direct measurement of $^1O_2$ luminescence, respectively.

Materials and Methods

Chemicals

Reagents and solvents were obtained commercially and used without further purification. The contents of one 100 μg vial of SOSG (Invitrogen, Eugene, OR, USA) were dissolved in 330 μL deoxygenated methanol to make a stock solution of 500 μM and stored at 4 °C in the dark.

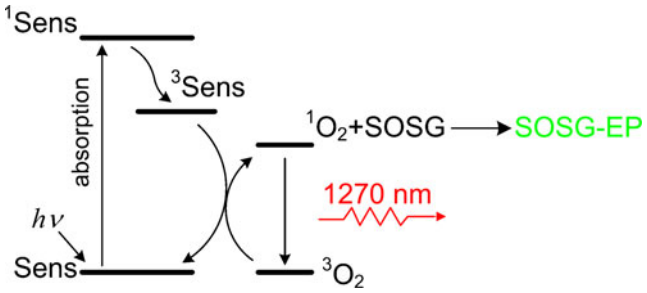

Fig. 1 Photooxidation of SOSG in the presence of $^1O_2$

Aqueous solutions from this stock were prepared immediately before use. For generation of $^1O_2$, a 100 μM stock solution of RB (Sigma-Aldrich, St. Louis, MO, USA) and HMME (Red-Green Photosensitizer Co., Ltd., Shanghai, China) were made up in initially air-statured phosphate buffered saline (PBS) at pH 7.5 and stored at 4 °C in the dark. Solutions of RB and HMME were prepared with an absorbance less than 0.20 at the desired wavelengths that are used in this study. Preparation was done in near-dark conditions to prevent photosensitized degradation of SOSG, RB and HMME.

Absorption and Fluorescence Spectroscopy

The absorption spectra of SOSG, RB and HMME in PBS were measured at room temperature in a UV/Vis/NIR spectrophotometer (Lambda 950, Perkin Elmer, Waltham, MA, USA) using a standard 10 mm pathlength quartz cuvette (101-QS, Hellma, Müllheim, GER). A spectrofluorimeter (FLS920, Edinburgh Instruments Ltd., Livingston, UK) was used for fluorescence measurements, keeping the slit widths constant at 2 nm for excitation and 0.5 nm for emission and integrating the signal for 0.3 s.

$^1O_2$ Generation from RB Photosensitization

A Xe arc lamp (XBO 450W/PFR, Osram, Munich, GER) with the wavelength selected by a monochromator in FLS920 was used to irradiate the RB for $^1O_2$ generation. An incident light beam with a power density of 7.5 mW/cm^2 was coupled directly into the cell holder of FLS920. The 2 mL samples were continuously and gently stirred during measurements to yield a homogeneous distribution of the molecules by mounting the cuvette on magnetic stirrer unit (VARIOMAG MINI, H+P Labortechnik AG, Bayern, Munich, GER). The cuvette was open to room air at the top. The irradiation time was precisely controlled with an exposure timer (GSZ-92A, Tianjin GangDong Scientific and Technical Development Co. Ltd., Tianjin, China).

SOSG Oxidation in the Presence of $^1O_2$

The reaction of SOSG with $^1O_2$ generated by photoirradiation of RB in PBS was investigated. The concentrations of SOSG and RB in the PBS solutions were varied in the ranges 0.125–10.00 μM and 0.25–1.00 μM, respectively. The fluorescence spectra were measured under 488 nm excitation in the range 495–701 nm in 2 nm steps, using a 495 nm long-pass filter (FGL495, ThorLabs, Newton, NJ, USA). A complete spectrum was measured in 45 s, and the measurements were repeated at 30 s intervals. The irradiation light was blocked by the shutter in the exposure timer while the fluorescence spectrum was being recorded.

Quantitative Measurements of $^1O_2$ Using SOSG

Fixing the concentration of RB in aqueous solution, the reaction rate (r) of SOSG with $^1O_2$ can be obtained by using the data of time-dependent fluorescence enhancement of SOSG, which is proportional to the concentration of SOSG-EP:

$$r=\frac{d[\mathrm{SOSG}-\mathrm{EP}]}{dt}=k[\mathrm{SOSG}]^n\left[^1\mathrm{O}_2\right], \quad (1)$$

where [SOSG-EP] is the concentration of SOSG-EP; [SOSG] and $[^1O_2]$ are the concentration of SOSG and $^1O_2$, respectively; n is the order of reaction with respect to SOSG. When n equals zero, r is only dependent upon $[^1O_2]$. In this case, we define the reaction of SOSG with $^1O_2$ as "n-zero reaction". As a result, the concentration of $^1O_2$ generated by photosensitization of RB can be quantitatively determined from the reaction rate (r).

In order to determine the minimal concentration of SOSG to meet the condition of n-zero reaction, various concentrations of SOSG have been used to react with $^1O_2$ generated by 1.00 μM RB photoirradiation in PBS. Furthermore, measurements were performed to explore the feasibility of quantitative measurement for $^1O_2$ generation from photosensitization of various RB concentrations by keeping the SOSG concentration constant. As demonstrated in previously studies, the reaction rate of the $^1O_2$ fluorescence probes oxidation by $^1O_2$ can be determined from the initial region of the kinetic curve, which allows the quantitation of $^1O_2$ generation [12, 13]. Therefore, as an additional test, the $^1O_2$ quantum yield of the porphyrin-based photosensitizer HMME was estimated by comparing the reaction rate of a known photosensitizer using SOSG after photosensitization in PBS. In this study, the $^1O_2$ quantum yield of HMME was determined, with respect to RB as a standard photosensitizer as following [28]:

$$\Phi_{\Delta HMME}=\frac{r_{HMME}/A_{HMME}}{r_{RB}/A_{RB}}\cdot\Phi_{\Delta RB}, \quad (2)$$

where r_{HMME} and r_{RB} are the reaction rate of the SOSG with $^1O_2$ generated from photosensitization of HMME and RB, respectively. A_{HMME} and A_{RB} are the absorbance of HMME and RB, respectively, and $\Phi_{\Delta RB}$ (0.76) is the $^1O_2$ quantum yield of RB.

Determination $^1O_2$ Quantum Yield of HMME by Measuring $^1O_2$ Luminescence

The main procedure for the measurement of $^1O_2$ quantum yield is based on the comparison of $^1O_2$ luminescence counts (λ_{max}=1270 nm) photosensitized by standard RB and HMME under the same conditions. To investigate this, the detection of time- and spectra-resolved of the $^1O_2$ luminescence was achieved by using our custom-developed high sensitive detection system, which has been described in detail elsewhere [29]. In briefly, the $^1O_2$ luminescence was detected by the NIR-PMT at an operating voltage of −900 V. Three NIR band-pass filters (1230, 1270, 1310 nm) were placed sequentially in front of the PMT to sample the $^1O_2$ luminescence spectrum. $^1O_2$ luminescence measurements were made continuously during irradiation of the sample by sampling each of the 1230, 1270 and 1310 nm filters in turn. In order to achieve a sufficient signal-to-noise ratio (SNR), the $^1O_2$ luminescence counts at each wavelength were summed over 285, 000 laser pulses. The $^1O_2$ luminescence for photosensitizers in PBS was corrected for background by subtracting the control sample of PBS alone, and the $^1O_2$ luminescence counts was determined as following:

$$I_{1270}=\left(I^S_{1270}-I^C_{1270}\right)-\left[\frac{\left(I^S_{1230}-I^C_{1230}\right)+\left(I^S_{1310}-I^C_{1310}\right)}{2}\right], \quad (3)$$

where I^S_{1270}, I^S_{1230} and I^S_{1310} are the luminescence counts with 1270, 1230 and 1310 nm filters for the photosensitizers, and I^C_{1270}, I^C_{1230} and I^C_{1310} are the corresponding counts for the control sample. The 1230 and 1310 nm filters, which lie outside the $^1O_2$ emission band, were used to determine the luminescence background in the 1270 nm region.

Based on the above measurements, the $^1O_2$ quantum yield of HMME can be determined, as previously reported [30]:

$$\Phi_{\Delta HMME}=\frac{I_{HMME}/A_{HMME}}{I_{RB}/A_{RB}}\cdot\frac{\tau_{\Delta RB}}{\tau_{\Delta HMME}}\cdot\Phi_{\Delta RB}, \quad (4)$$

where I_{HMME} and I_{RB} are the integration photon counts from 0.5 to 20 μs in the time-resolved $^1O_2$ luminescence spectra of HMME and RB, respectively. $\tau_{\Delta HMME}$ and $\tau_{\Delta RB}$ are the $^1O_2$ lifetimes of HMME and RB, respectively.

Statistical Analysis

The data were processed and graphed using Origin8.0 software (OriginLab Corporation, Northampton, MA, USA), and all values are presented as means ± the standard deviation (SD) for three independent samples.

Results and Discussion

Optimal Irradiation Wavelength for $^1O_2$ Generation

Figure 2 shows the normalized absorption spectra of the RB, HMME and SOSG in PBS solution. It is evident that the absorption region of SOSG is up to 550 nm. Recently,

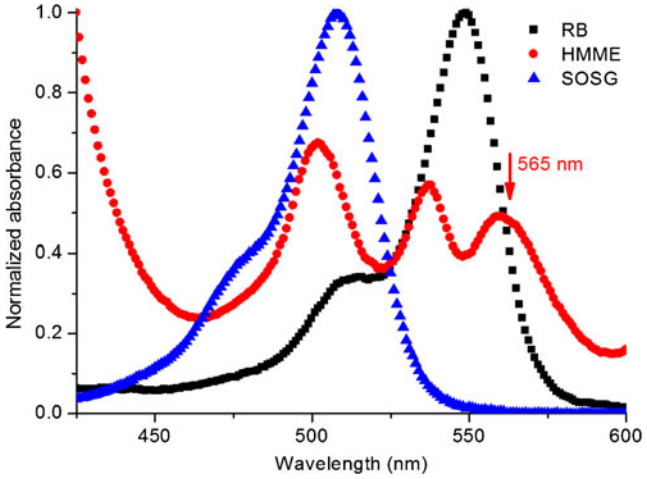

Fig. 2 Normalized absorption spectra of RB, HMME and SOSG in PBS solution

Ragàs et al. noticed that the SOSG is able to produce $^1O_2$ by itself under exposure to ultraviolet and visible radiation, and the photo-induced production of $^1O_2$ by SOSG is dependent on the irradiation wavelengths and the different reaction pathways [31]. In order to avoid the potential absorption of SOSG during photoirradiation, the irradiation wavelength of 565 nm was selected for $^1O_2$ generation in this study. As indicated in Fig. 2, the absorption of exciting light at 565 nm is almost exclusively for SOSG, while the desired absorption of light for RB and HMME can be obtained.

SOSG Oxidation in the Presence of $^1O_2$

$^1O_2$ generation from the irradiation of RB in PBS was monitored by using SOSG as a fluorescence probe. Figure 3a shows the fluorescence emission spectra from RB itself, SOSG and a mixture of RB+SOSG at equimolar concentrations, before and after photoirradiation. The appearance of intrinsic fluorescence upon excitation of the SOSG itself in PBS at 488 nm was observed, even in the absence of external $^1O_2$ generation, as shown in Fig. 3a. Note that the maximal fluorescence signal at 531 nm can be reliably measured in this system down to about 0.125 μM (data not shown), which is important when SOSG is used for the measurement of extremely low $^1O_2$ generation. This finding is consistent with a number of previous observations that SOSG initially exhibits a relatively weak emission around 530 nm [16]. RB has a maximum fluorescence emission peak at 565 nm, while its emission at 531 nm is negligible compared to that of SOSG. There is no evident chemical reaction between the RB and SOSG without irradiation, since the intrinsic spectra are unchanged and additive. Upon irradiation, the green fluorescence intensity in the mixture solution of RB+SOSG continuously increased with the irradiation time, representing the generation of $^1O_2$

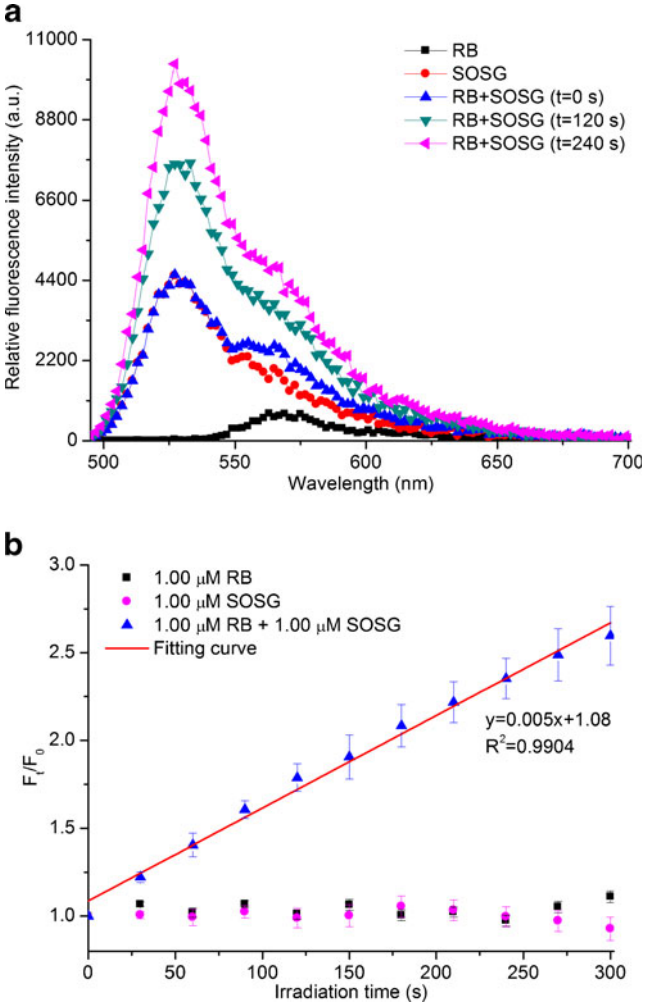

Fig. 3 Fluorogenic interactions between 1.00 μM SOSG and $^1O_2$ generated by photoirradiation of 1.00 μM RB. Fluorescence excited at 488 nm. **a** Fluorescence emission spectra of RB and SOSG before irradiation and a mixture of RB+SOSG before and at two different time points after irradiation. **b** Dependence of the fluorescence enhancement of F_t/F_0 on irradiation time

during the irradiation and much higher fluorescence of SOSG-EP compared to SOSG. In contrast, the three control samples (including 1.00 μM RB, SOSG, and a mixture of RB+SOSG at equimolar concentrations without irradiation) showed negligible fluorescence intensity changes (data not shown). As shown in Fig. 3b, there is a good linear relationship between the green fluorescence enhancement of F_t/F_0, with the irradiation time for the mixture of RB+SOSG, where F_0 and F_t are the fluorescence intensity before and after irradiation. However, no significant fluorescence enhancement with 488 nm excitation was observed from the emission of RB or SOSG alone at 565 and 531 nm, respectively. This finding implies that the increased fluorescence intensity is caused only from the $^1O_2$ generation of RB, and the alteration of light absorption by SOSG and RB can be negligible during the measurements.

Quantitative Measurement of $^1O_2$ Generation with SOSG

Fixing the RB concentration at 1.00 μM, Fig. 4a shows this over a wide range of SOSG concentration, from 0.25 to 10.00 μM. The green fluorescence intensity increases linearly with irradiation time, up to at least 300 s. Meanwhile, there is no significant photobleaching of RB or SOSG was observed during the measurements (data not shown). In this case, the reaction rate (r) of the SOSG with $^1O_2$ can be determined from the slope of the linear curve. As indicated in Fig. 4b, r increases with the initial SOSG concentration, but reaching plateau at above 6.00 μM SOSG. Next, the natural logarithm of r was plotted against the natural logarithm of [SOSG]. According to the Eq. (1), the slopes of the curves represent the reaction order of SOSG (n). As shown in Fig. 4c, when [SOSG] great than or equal to 6.00 μM, n reaches to zero. Therefore, when the RB concentration is less than 1.00 μM, the current measurements suggest that 6.00 μM SOSG is sufficient for achieving n-zero reaction and can be treated as constant.

Furthermore, the n-zero reaction for 6.00 μM SOSG reacting with $^1O_2$ that generated from RB and HMME photosensitization were compared studies. Figure 5a and b show the reaction kinetic curves (curve slope, which is paralleling the formation rate of SOSG-EP) are increased with the increase in photosensitizer concentrations of RB and HMME, respectively. In an effort to obtain the rate of SOSG-EP formation in this reaction, the correlation between photosensitizer absorbance and the rate of fluorescence enhancement was further examined. As shown in Fig. 5c, the r shows a very good linear relationship with the RB and HMME absorbance, with the slope values of 3160±19 and 511±17 (arbitrary unit) s^{-1}, respectively. In this case, the $^1O_2$ quantum yield of HMME in PBS can be calculated to be 0.12±0.01 with Eq. 2. This finding suggests that the SOSG reaction with $^1O_2$ is n-zero reaction with respect to the photosensitizer concentrations, and that the $^1O_2$ generation in this reaction can be quantitatively determined by using SOSG as a fluorescent reporter. However, the reaction between SOSG and $^1O_2$ was shown to be sensitive to the pH, temperature, dissolved oxygen concentration, and so on, thus further care should be exercised when using SOSG as a $^1O_2$ probe for quantitative measurements in a specific microenvironment [32].

Determination $^1O_2$ Quantum Yield of HMME by Measuring $^1O_2$ Luminescence

Figure 6a shows the time-resolved $^1O_2$ luminescence curves for various concentrations of RB and HMME in PBS, respectively. Based on the previously established method [29], the triplet state and $^1O_2$ lifetimes of HMME were derived by fitting the obtained $^1O_2$ luminescence spectra in Fig. 6a. The $^1O_2$ lifetimes of RB and HMME have similar values of 4.31± 0.03 and 4.00±0.04 μs, respectively, which are consistent with the newly published literature values [33]. As shown in Fig. 6b, the $^1O_2$ luminescence intensities of RB and HMME show a linear dependence on their absorbance, as expected.

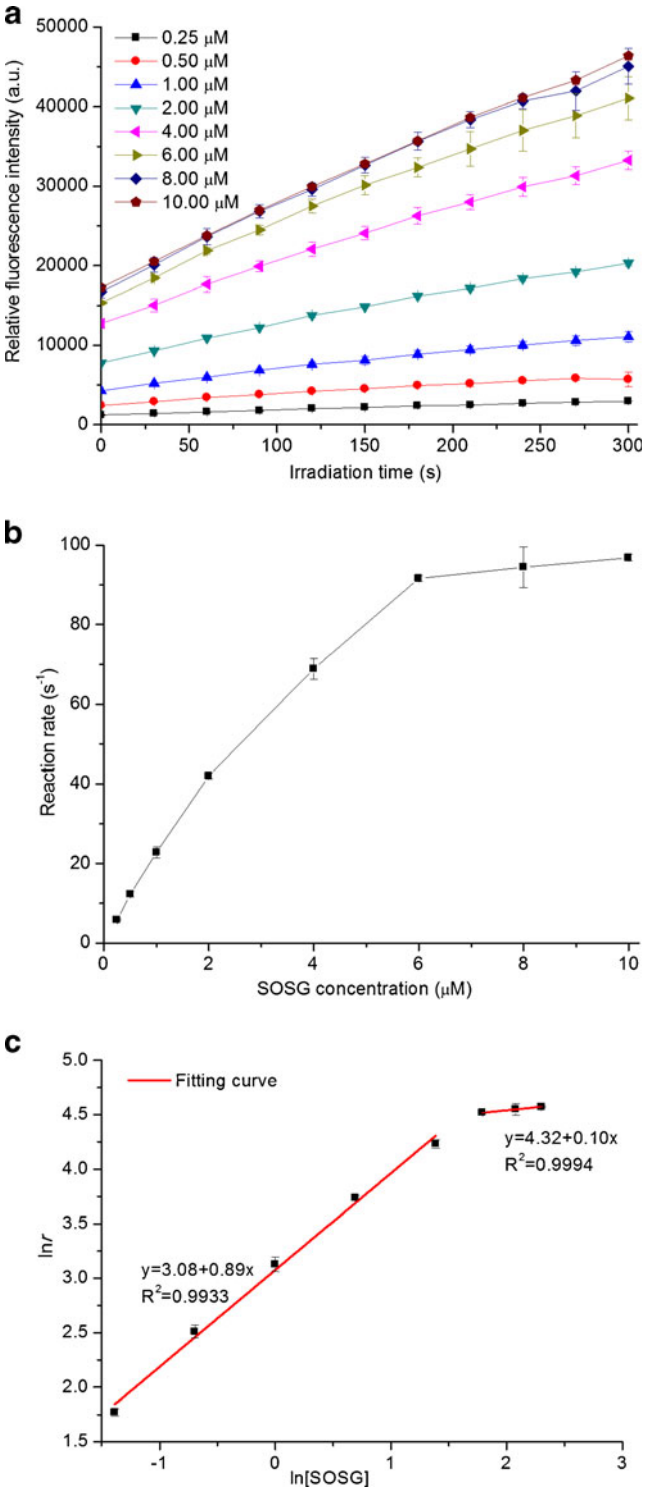

Fig. 4 Reaction kinetics for SOSG with $^1O_2$ generation from photoirradiation of 1.00 μM RB solution. **a** Reaction of different concentrations of SOSG with $^1O_2$ generation. **b** Reaction rates versus SOSG concentration. **c** ln[r] versus ln[SOSG]

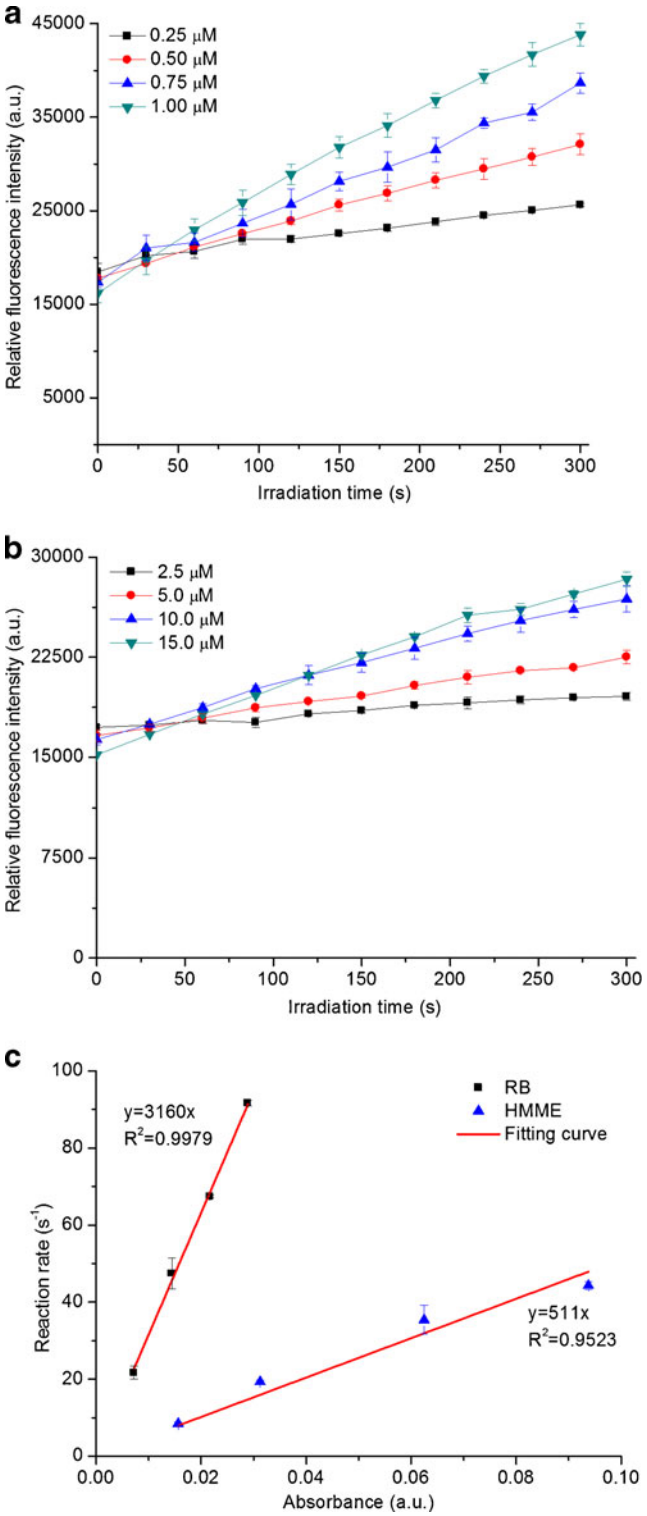

Fig. 5 Quantitative measurements for $^1O_2$ generation using SOSG as the reporter probe. **a** Reaction of 6.00 μM SOSG with $^1O_2$ generation from different concentrations of RB. **b** Reaction of 6.00 μM SOSG with $^1O_2$ generation from different concentrations of HMME. **c** Reaction rates as a function of RB and HMME absorbance

According to the Eq. 4, the $^1O_2$ quantum yield of HMME can be determined to be 0.13. This value is in good agreement

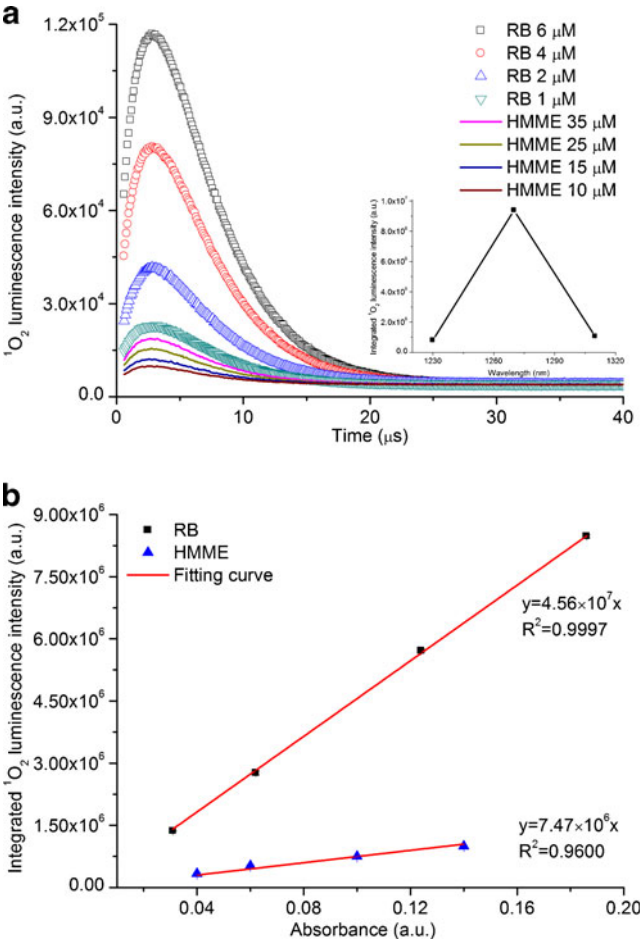

Fig. 6 Direct measurement of $^1O_2$ luminescence intensity. **a** Time-resolved $^1O_2$ luminescence spectra of RB and HMME for different concentration. A typical spectral-resolved $^1O_2$ luminescence spectrum is shown in inset. **b** Integrated $^1O_2$ luminescence counts against absorbance for RB and HMME

with the value obtained above by using SOSG, which implies that the $^1O_2$ generation estimated from steady-state measurements on the enhanced fluorescence is reliable as well as that from the time-resolved $^1O_2$ luminescence measurements. Hence, the quantitative measurement of $^1O_2$ generation using SOSG as a fluorescent reporter is not only feasible but also accurate.

Conclusions

The application of SOSG as a fluorescence probe for quantitative monitoring of $^1O_2$ generation has been demonstrated in photoirradiation of RB and HMME solutions. $^1O_2$ reacts with SOSG to produce SOSG-EP that emits green fluorescence with a maximum at 531 nm. It is evident that the fluorescence intensity of SOSG-EP depends on the initial concentrations of SOSG and photosensitizers, and the photoirradiation time for $^1O_2$ generation. The feasibility for quantitative measurement

of $^1O_2$ generation by using SOSG has been demonstrated here for the first time: this can be achieved directly by determining the reaction rate in the condition of the order of reaction with respect to SOSG equals zero. Furthermore, the obtained $^1O_2$ quantum yield of porphyrin-based photosensitizer HMME in PBS by using SOSG is in good agreement with the value that independently determined by using direct measurement of $^1O_2$ luminescence.

Acknowledgements This work was supported by the National Natural Science Foundation of China (60978070), the program for New Century Excellent Talents in University of China (NCET-10-0012), the Fujian Provincial Natural Science Foundation (2011J01342, 2011J06022) and the Program for Changjiang Scholars and Innovative Research Team in University (IRT1115). BW acknowledges the support of the Canadian Cancer Society Research Institute for research in PDT dosimetry.

References

1. Mitsunaga M, Ogawa M, Kosaka N, Rosenblum LT, Choyke PL, Kobayashi H (2011) Cancer cell-selective in vivo near infrared photoimmunotherapy targeting specific membrane molecules. Nat Med 17(12):1685–1691
2. Driever SM, Fryer MJ, Mullineaux PM, Baker NR (2009) Imaging of reactive oxygen species in vivo. Methods Mol Biol 479:109–116
3. Triantaphylides C, Havaux M (2009) Singlet oxygen in plants: production, detoxification and signaling. Trends Plant Sci 14(4):219–228
4. Jarvi MT, Niedre MJ, Patterson MS, Wilson BC (2006) Singlet oxygen luminescence dosimetry (SOLD) for photodynamic therapy: current status, challenges and future prospects. Photochem Photobiol 82(5):1198–1210
5. Li BH, Wilson BC (2011) Direct and indirect measurements of singlet oxygen for photodynamic therapy. Proceedings 13th International Photodynamic Association World Congress pp 43–47
6. Kessel D, Price M (2012) Evaluation of DADB as a probe for singlet oxygen formation during photodynamic therapy. Photochem Photobiol 88(3):717–720
7. Chen X, Tian X, Shin I, Yoon J (2011) Fluorescent and luminescent probes for detection of reactive oxygen and nitrogen species. Chem Soc Rev 40(9):4783–4804
8. Oliveira MS, Severino D, Prado FM, Angeli JP, Motta FD, Baptista MS, Medeiros MH, Di Mascio P (2011) Singlet molecular oxygen trapping by the fluorescent probe diethyl-3,3′-(9,10-anthracenediyl)-bisacrylate synthesized by the Heck reaction. Photochem Photobiol Sci 10(10):1546–1555
9. Jimenez-Banzo A, Ragas X, Kapusta P, Nonell S (2008) Time-resolved methods in biophysics. 7. Photon counting vs. analog time-resolved singlet oxygen phosphorescence detection. Photochem Photobiol Sci 7(9):1003–1010
10. Niedre MJ, Patterson MS, Giles A, Wilson BC (2005) Imaging of photodynamically generated singlet oxygen luminescence in vivo. Photochem Photobiol 81(4):941–943
11. Umezawa N, Tanaka K, Urano Y, Kikuchi K, Higuchi T, Nagano T (1999) Novel fluorescent probes for singlet oxygen. Angew Chem Int Ed Engl 38(19):2899–2901
12. Tanaka K, Miura T, Umezawa N, Urano Y, Kikuchi K, Higuchi T, Nagano T (2001) Rational design of fluorescein-based fluorescence probes. Mechanism-based design of a maximum fluorescence probe for singlet oxygen. J Am Chem Soc 123(11):2530–2536
13. Song B, Wang GL, Tan MQ, Yuan JL (2006) A europium(III) complex as an efficient singlet oxygen luminescence probe. J Am Chem Soc 128(41):13442–13450
14. Singlet Oxygen Sensor Green Reagent (Invitrogen, Eugene, 2004) pp 1–2
15. Gollmer A, Arnbjerg J, Blaikie FH, Pedersen BW, Breitenbach T, Daasbjerg K, Glasius M, Ogilby PR (2011) Singlet Oxygen Sensor Green (R): photochemical behavior in solution and in a mammalian cell. Photochem Photobiol 87(3):671–679
16. Flors C, Fryer MJ, Waring J, Reeder B, Bechtold U, Mullineaux PM, Nonell S, Wilson MT, Baker NR (2006) Imaging the production of singlet oxygen in vivo using a new fluorescent sensor, singlet oxygen sensor green. J Exp Bot 57(8):1725–1734
17. Ragas X, Cooper LP, White JH, Nonell S, Flors C (2011) Quantification of photosensitized singlet oxygen production by a fluorescent protein. Chemphyschem 12(1):161–165
18. Hideg E (2008) A comparative study of fluorescent singlet oxygen probes in plant leaves. Cent Eur J Biol 3(3):273–284
19. Zhang Y, Aslan K, Previte MJ, Geddes CD (2008) Plasmonic engineering of singlet oxygen generation. Proc Natl Acad Sci U S A 105(6):1798–1802
20. Zhang Y, Aslan K, Previte MJR, Geddes CD (2007) Metal-enhanced singlet oxygen generation: a consequence of plasmon enhanced triplet yields. J Fluoresc 17(4):345–349
21. Hotze EM, Badireddy AR, Chellam S, Wiesner MR (2009) Mechanisms of bacteriophage inactivation via singlet oxygen generation in UV illuminated fullerol suspensions. Environ Sci Technol 43 (17):6639–6645
22. Tam TT, Juzeniene A, Steindal AH, Iani V, Moan J (2009) Photodegradation of 5-methyltetrahydrofolate in the presence of Uroporphyrin. J Photochem Photobiol B 94(3):201–204
23. Yan F, Zhang Y, Yuan HK, Gregas MK, Vo-Dinh T (2008) Apoferritin protein cages: a novel drug nanocarrier for photodynamic therapy. Chem Commun 14(38):4579–4581
24. Price M, Reiners JJ, Santiago AM, Kessel D (2009) Monitoring singlet oxygen and hydroxyl radical formation with fluorescent probes during photodynamic therapy. Photochem Photobiol 85(5):1177–1181
25. Yan F, Zhang Y, Kim KS, Yuan HK, Vo-Dinh T (2010) Cellular uptake and photodynamic activity of protein nanocages containing methylene blue photosensitizing drug. Photochem Photobiol 86(3):662–666
26. Shen Y, Lin HY, Huang ZF, Chen DF, Li BH, Xie SS (2011) Indirect imaging of singlet oxygen generation from a single cell. Laser Phys Lett 8(3):232–238
27. Redmond RW, Gamlin JN (1999) A compilation of singlet oxygen yields from biologically relevant molecules. Photochem Photobiol 70(4):391–475
28. Wilkinson F, Helman WP, Ross AB (1993) Quantum yields for the photosensitized formation of the lowest electronically excited singlet state of molecular oxygen in solution. J Phys Chem Ref Data 22(1):113–262
29. Lin HY, Chen DF, Shen Y, Li BH, Xie SS (2011) The influence of pulse-height discrimination threshold on the accuracy of singlet oxygen luminescence measurements. J Optics 13(12):125301
30. Li BH, Lin LS, Lin HY, Xie SS (2008) Singlet oxygen quantum yields of porphyrin-based photosensitizers for photodynamic therapy. J Innovation Opt Health Sci 1(1):141–149
31. Ragas X, Jimenez-Banzo A, Sanchez-Garcia D, Batllori X, Nonell S (2009) Singlet oxygen photosensitisation by the fluorescent probe Singlet Oxygen Sensor Green. Chem Commun 28(20):2920–2922
32. Swanson SJ, Choi WG, Chanoca A, Gilroy S (2011) In vivo imaging of Ca(2+), pH, and reactive oxygen species using fluorescent probes in plants. Annu Rev Plant Biol 62(62):273–297
33. Lee S, Zhu L, Minhaj AM, Hinds MF, Vu DH, Rosen DI, Davis SJ, Hasan T (2008) Pulsed diode laser-based monitor for singlet molecular oxygen. J Biomed Opt 13(3):034010